

Original Article

Efficacy of Flaxseed Compared to ACE Inhibition in Treating Anthracycline- and Trastuzumab-Induced Cardiotoxicity

Sara M. Telles-Langdon, BKin (Hons), MSc,^a Vibhuti Arya, BSc (Hons), MSc,^a Paris R. Haasbeek,^b David Y.C. Cheung, BSc,^a Cameron R. Eekhoudt, BSc, MSc,^a Lana Mackic, BSc,^a Ashley N. Bryson, BSc, MD,^a Sonu S. Varghese, BSc, MSc,^a J. Alejandro Austria,^a James A. Thliveris, PhD,^c Harold M. Aukema, PhD,^d Amir Ravandi, MD, PhD, FRCPC,^{a,e} Pawan K. Singal, PhD, DSc, LLD (Hon),^a and Davinder S. Jassal, MD, FACC, FCCS, FRCPC^{a,e,f}

^a Institute of Cardiovascular Sciences, Department of Physiology and Pathophysiology, Max Rady College of Medicine, Rady Faculty of Health Sciences, University of Manitoba, Winnipeg, Manitoba, Canada

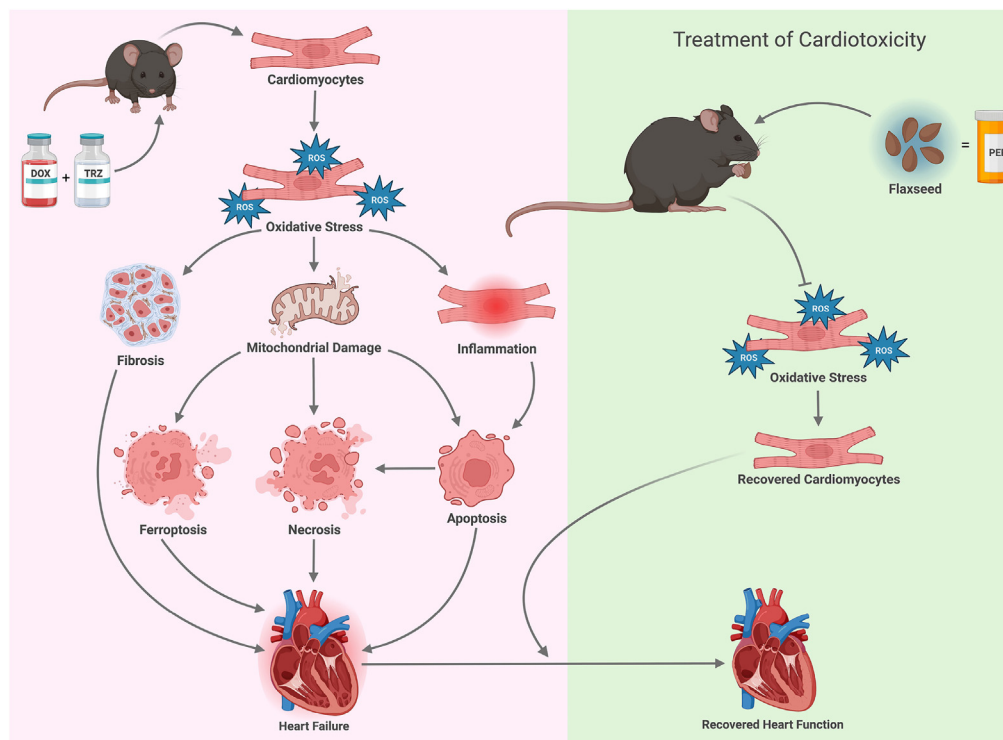
^b Faculty of Science, University of Manitoba, Winnipeg, Manitoba, Canada

^c Department of Human Anatomy and Cell Sciences, Max Rady College of Medicine, Rady Faculty of Health Sciences, University of Manitoba, Winnipeg, Manitoba, Canada

^d Canadian Centre for Agri-Food Research in Health and Medicine, Department of Food and Nutritional Sciences, Faculty of Agriculture and Food Sciences, University of Manitoba, Winnipeg, Manitoba, Canada

^e Section of Cardiology, Department of Internal Medicine, Max Rady College of Medicine, Rady Faculty of Health Sciences, University of Manitoba, Winnipeg, Manitoba, Canada

^f Department of Radiology, Max Rady College of Medicine, Rady Faculty of Health Sciences, University of Manitoba, Winnipeg, Manitoba, Canada



ABSTRACT

Background: Although the current combination of surgery, radiation, and chemotherapy is used in the breast-cancer setting, the administration of the anticancer drugs doxorubicin and trastuzumab is associated with an increased risk of developing heart failure. The aim of this study is to determine whether dietary flaxseed is comparable and/or synergistic with the angiotensin-converting enzyme inhibitor perindopril in the treatment of doxorubicin- and trastuzumab-mediated cardiotoxicity.

Methods: In a chronic *in vivo* murine model (n = 110), doxorubicin and trastuzumab (8 mg/kg and 3 mg/kg, respectively) were administered weekly for 3 weeks. Following this period, the mice were randomized to daily consumption of a 10% flaxseed supplemented diet, administration of perindopril (3 mg/kg) via oral gavage, or a combination of both flaxseed and perindopril for an additional 3 weeks.

Results: In mice treated with doxorubicin and trastuzumab, the left ventricular ejection fraction decreased from 74% ± 4% at baseline to 30% ± 2% at week 6. Treatment with either flaxseed or perindopril, or with flaxseed and perindopril improved left ventricular ejection fraction to 52% ± 4%, 54% ± 4%, and 55% ± 3%, respectively (P < 0.05). Although histologic analyses confirmed significant loss of sarcomere integrity and vacuolization in the doxorubicin- and trastuzumab-treated mice, treatment with flaxseed or perindopril, or with flaxseed and perindopril improved myocyte integrity. Finally, the level of Bcl-2 interacting protein 3, high-mobility group box 1 protein expression, and the levels of select oxylipins, were significantly elevated in mice receiving doxorubicin and trastuzumab; these markers were attenuated by treatment with either flaxseed or perindopril, or with flaxseed and perindopril.

Conclusions: Flaxseed was equivalent to perindopril at improving cardiovascular remodelling by reducing biomarkers of inflammation, mitochondrial damage, and cell death.

RÉSUMÉ

Contexte : Si l'association actuelle de la chirurgie, de la radiothérapie et de la chimiothérapie est utilisée pour le traitement du cancer du sein, on observe néanmoins que l'administration de la doxorubicine et du trastuzumab, deux anticancéreux, augmente les risques d'insuffisance cardiaque. Cette étude vise à déterminer si les graines de lin alimentaires ont un effet comparable et/ou synergique à celui du péridopril, un inhibiteur de l'enzyme de conversion de l'angiotensine, dans le traitement de la cardiotoxicité liée à la doxorubicine et au trastuzumab.

Méthodologie : Dans un modèle murin chronique *in vivo* (n = 110), la doxorubicine et le trastuzumab (8 mg/kg et 3 mg/kg, respectivement) ont été administrés une fois par semaine pendant trois semaines. Après cette période, les souris ont été réparties de façon aléatoire dans trois groupes : l'un recevant tous les jours un régime alimentaire contenant 10 % de graines de lin, un autre recevant du péridopril (3 mg/kg) par gavage oral et un troisième recevant à la fois des graines de lin et du péridopril pendant trois semaines supplémentaires.

Résultats : Chez les souris recevant la doxorubicine et le trastuzumab, la fraction d'éjection ventriculaire gauche est passée de 74 % ± 4 % au départ à 30 % ± 2 % à la semaine 6. Avec le traitement par les graines de lin seules, le péridopril seul ou les graines de lin et le péridopril en association, la fraction d'éjection ventriculaire gauche est passée à 52 % ± 4 %, à 54 % ± 4 % et à 55 % ± 3 %, respectivement (p < 0,05). Bien que les analyses histologiques aient permis de confirmer une perte significative de l'intégrité des sarcomères et une vacuolisation chez les souris recevant la doxorubicine et le trastuzumab, le traitement par les graines de lin seules, le péridopril seul ou les graines de lin et le péridopril en association a amélioré l'intégrité des myocytes. Enfin, les taux de protéine 3 interagissant avec BCL-2, l'expression de la protéine HMGB1 (*high-mobility group box 1*) et les taux de certaines oxylipines étaient significativement élevés chez les souris recevant la doxorubicine et le trastuzumab. Ces marqueurs ont été atténués par les graines de lin, le péridopril ou l'association des deux.

Conclusions : En diminuant les biomarqueurs de l'inflammation, les dommages aux mitochondries et la mort cellulaire, les graines de lin ont un effet équivalent à celui du péridopril quant à l'amélioration du remodelage cardiovasculaire.

The field of cardio-oncology focuses on the prevention, diagnosis, and management of cancer patients who are at risk of developing cardiovascular complications as a result of their underlying treatment. For early-stage breast cancer, the most frequently prescribed chemotherapy regimens include anthracyclines, specifically doxorubicin (DOX).^{1,2} Although these regimens are effective in reducing the overall incidence of morbidity and mortality in the breast-cancer setting, the use of anthracyclines is associated with a 10% dose-dependent risk

of developing cardiotoxicity.^{3,4} Targeted biological therapies are a complementary approach to cancer treatment, blocking cancer-promotive properties of specific hormone or protein receptors. Trastuzumab (TRZ) is a monoclonal antibody that specifically inhibits the human epidermal growth factor receptor 2 in the breast-cancer setting.⁴⁻⁶ When used in conjunction with anthracyclines, however, TRZ increases the rate of chemotherapy-induced cardiotoxicity to 25%.^{7,8} The mechanistic pathways involved in DOX + TRZ-mediated cardiotoxicity are multifactorial and include increased inflammation, oxidative stress, apoptosis, necrosis, and/or ferroptosis.⁹⁻¹⁴

Cardiac dysfunction is the leading cause of morbidity and mortality among cancer survivors.¹⁵ To standardize the diagnostic criteria for cancer therapy-related cardiac dysfunction (CTRC), the Canadian Cardiovascular Society developed the defining parameters as a > 10% decrease in left ventricular ejection fraction (LVEF), compared to baseline, or an absolute LVEF of < 53%

Received for publication January 9, 2024. Accepted March 15, 2024.

Corresponding author: Dr Davinder S. Jassal, Professor of Medicine, Radiology, and Physiology and Pathophysiology, Section of Cardiology, Department of Internal Medicine, Max Rady College of Medicine, Rady Faculty of Health Sciences, University of Manitoba, Rm Y3531, Bergen Cardiac Care Centre, St. Boniface Hospital, 409 Tache Avenue, Winnipeg, Manitoba R2H 2A6, Canada. Tel.: +1-204-258-1290; fax: +1-204-233-2157.

E-mail: djassal@sbgh.mb.ca

See page 935 for disclosure information.

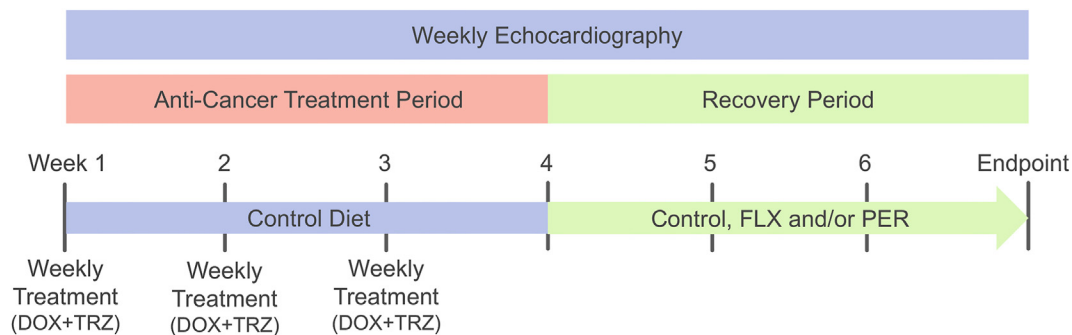


Figure 1. Experimental timeline. Mice were randomized into control or the doxorubicin and trastuzumab (DOX + TRZ) anticancer treatment group receiving the following: (i) 0.9% saline (n = 16); or (ii) 8 mg/kg DOX + 3 mg/kg TRZ (n = 94) administered at the start of weeks 1, 2, and 3 via intraperitoneal injection, to establish a chronic *in vivo* murine model of chemotherapy-induced cardiotoxicity. Mice were randomized further, to receive *ad libitum* access to their respective diets and perindopril (PER) or water via oral gavage for weeks 4 through 6. Cardiac function was assessed weekly using transthoracic echocardiography. FLX, flaxseed.

following chemotherapy treatment.¹⁶ Upon detection of CTRCD, the anticancer agents are temporarily discontinued, and an angiotensin-converting enzyme inhibitor (ACEi) and a beta-adrenergic receptor blocker (β -blocker) are introduced, with the goal of reversing the chemotherapy-mediated cardiotoxicity.¹⁶⁻¹⁸

In addition to pharmaceuticals, the role of nutraceuticals is an evolving area of research in the field of cardio-oncology. Flaxseed (FLX), in addition to its basic nutritional function, has been shown to have a positive health effect in several disease conditions, including cancer and cardiovascular disease.^{19,20} The physiologically active nutraceutical components of FLX include anti-inflammatory alpha-linoleic acid (ALA) and the antioxidant secoisolariciresinol diglucoside (SDG). We recently demonstrated that prophylactic treatment with FLX, ALA, and SDG was partially cardioprotective in a chronic *in vivo* female mouse model of DOX + TRZ-mediated cardiotoxicity, and FLX offers equal cardioprotection to the ACEi perindopril (PER) in the preventative setting.^{20,21} Considering these findings, a reasonable hypothesis is that FLX may be efficacious, in not only the prevention,^{20,21} but also the treatment of established DOX + TRZ-mediated cardiotoxicity, through its anti-inflammatory and antioxidant properties.

The objective of the current study is to evaluate whether FLX is comparable to and/or incremental to standard pharmacologic therapy using the ACEi PER in the treatment of DOX + TRZ-mediated cardiotoxicity in a chronic *in vivo* murine model.

Methods

Experimental animal model

A total of 110 wild-type C57Bl/6 female mice (aged 12-15 weeks; Jackson Laboratories, Bar Harbor, ME) were used. They had *ad libitum* access to water, and the study diets were maintained on a 12-hour day/night cycle in the animal holding facility. At weeks 1, 2, and 3, the mice received intraperitoneal (i.p.) injections with saline or DOX + TRZ (8 mg/kg and 3 mg/kg, respectively) in prespecified groups, to

create a chronic *in vivo* murine model of chemotherapy-induced cardiotoxicity, as previously described.²² Mice had *ad libitum* access to regular chow or a 10% FLX-supplemented (~ 0.5 g/d) diet, and they were administered PER (3 mg/kg/d) or a control via oral gavage on a daily basis, starting on week 4 and continuing until the study endpoint in the prespecified groups. All mice were subject to weight analysis and weekly transthoracic echocardiography throughout the study (Fig. 1). Blood pressure was measured at baseline, week 3, and week 6 in restrained, nonsedated mice using the noninvasive tail cuff method, as previously described.^{9,23-30}

Murine echocardiography

Serial transthoracic echocardiography was performed weekly to assess cardiac structure and left ventricular (LV) systolic function in a subset of mice, as previously described.^{9,23-30} Images acquired in the parasternal long-axis view were analyzed to calculate LVEF.^{31,32} Images acquired in the parasternal short-axis M-mode view were analyzed to measure heart rate, interventricular septal wall thickness, posterior wall thickness, and LV end-diastolic diameter (LVEDD).^{31,32}

Histologic analysis

Cardiac tissues were prepared for both light and electron microscopy in a subset of mice from each group. LV tissue for light microscopy was sectioned and preserved prior to paraffin embedding and imaging. Serial 5 μm -thick sections were cut from each paraffin block for dewaxing, rehydration, and Masson's trichrome staining. Digital images then were taken with identical exposure settings for all sections (n = 5).

LV tissue for electron microscopy was sectioned, cut into 0.5- mm^2 pieces, fixed, dehydrated, and embedded in Epon 812.³³ Tissue sections were stained with uranyl acetate and lead citrate. To avoid observer bias, grids were coded without prior knowledge of their source. Digital images then were taken with the Philips CM12 electron microscope, (Eindhoven, Netherlands) to determine the degree of cellular integrity (n = 5).

Table 1. Echocardiographic parameters of C57Bl/6 mice receiving saline or doxorubicin (DOX) + trastuzumab (TRZ), followed by daily treatment with flaxseed (FLX), perindopril (PER), or FLX + PER

Parameter	Group	Baseline	Week 6	P
HR, bpm	Control (n = 15)	690 ± 5	692 ± 4	0.88
	DOX + TRZ (n = 15)	699 ± 4	701 ± 6	0.91
	FLX + DOX + TRZ (n = 15)	686 ± 7	689 ± 5	0.84
	PER + DOX + TRZ (n = 15)	690 ± 5	685 ± 7	0.83
	FLX + PER + DOX + TRZ (n = 15)	688 ± 6	691 ± 4	0.85
IVS, mm	Control (n = 15)	0.81 ± 0.01	0.81 ± 0.02	0.93
	DOX + TRZ (n = 15)	0.82 ± 0.02	0.82 ± 0.03	0.92
	FLX + DOX + TRZ (n = 15)	0.81 ± 0.01	0.82 ± 0.01	0.92
	PER + DOX + TRZ (n = 15)	0.82 ± 0.01	0.82 ± 0.02	0.97
	FLX + PER + DOX + TRZ (n = 15)	0.81 ± 0.01	0.82 ± 0.01	0.89
PWT, mm	Control (n = 15)	0.82 ± 0.01	0.82 ± 0.02	0.91
	DOX + TRZ (n = 15)	0.81 ± 0.02	0.81 ± 0.03	0.90
	FLX + DOX + TRZ (n = 15)	0.81 ± 0.01	0.80 ± 0.01	0.91
	PER + DOX + TRZ (n = 15)	0.80 ± 0.01	0.81 ± 0.02	0.95
	FLX + PER + DOX + TRZ (n = 15)	0.82 ± 0.01	0.81 ± 0.01	0.92
LVEDD, mm	Control (n = 15)	2.8 ± 0.1	2.9 ± 0.1	0.89
	DOX + TRZ (n = 15)	2.9 ± 0.2	4.6 ± 0.2*	< 0.05
	FLX + DOX + TRZ (n = 15)	2.8 ± 0.2	3.8 ± 0.2*†	< 0.05
	PER + DOX + TRZ (n = 15)	2.9 ± 0.1	3.9 ± 0.2*†	< 0.05
	FLX + PER + DOX + TRZ (n = 15)	2.8 ± 0.2	3.8 ± 0.1*†	< 0.05
LVEF, %	Control (n = 15)	73 ± 3	74 ± 4	0.92
	DOX + TRZ (n = 15)	74 ± 4	30 ± 2*	< 0.05
	FLX + DOX + TRZ (n = 15)	74 ± 4	52 ± 4*†	< 0.05
	PER + DOX + TRZ (n = 15)	75 ± 3	54 ± 4*†	< 0.05
	FLX + PER + DOX + TRZ (n = 15)	73 ± 4	55 ± 3*†	< 0.05

Baseline and week 6 measures with *P*-values. Values other than *P*-values are presented as mean ± standard deviation.

HR, heart rate; IVS, interventricular septum; LVEDD, left ventricular end-diastolic diameter; LVEF, left ventricular ejection fraction; PWT, posterior wall thickness.

* *P* < 0.05, DOX + TRZ vs control.

† *P* < 0.05 FLX + DOX + TRZ or PER + DOX + TRZ or PER + FLX + DOX + TRZ vs DOX + TRZ & control.

Western blot analyses

LV tissue samples were flash frozen in liquid nitrogen, and then crushed and homogenized in a radio-immunoprecipitation assay lysis buffer containing phosphatase and protease inhibitor, for total cellular protein extraction. Protein concentrations were determined using a Bradford protein assay (Rockford, IL). Loading samples containing 30 µg of protein then were made for Western blot analysis. Western blot analysis was performed to quantify high-mobility group box 1 protein (HMGB1: biomarker of necrosis and mitochondrially mediated ferroptosis) and B-cell lymphoma 2 interacting protein 3 (Bnip-3: biomarker of mitochondrial damage, apoptosis, and necrosis) in a subset of mice. Western blot analysis also was performed to quantify nuclear factor kappa beta (NF-κβ), phospho-NF-κβ, poly-adenosine diphosphate (ADP)-ribose-polymerase (PARP), Bcl-2 associated X protein (Bax), B-cell lymphoma extra-large (Bcl-XL), and Caspase-3 in a subset of mice.

Samples were run in a 5% stacking and a 12% resolving sodium dodecyl sulfate polyacrylamide gel for protein separation, and subsequently, they were transferred to a polyvinylidene difluoride membrane. Once the proteins were transferred, the membranes were blocked using 5% skim milk powder, probed using 1/1000 rabbit-source target-specific primary antibodies, and standardized using a glyceraldehyde 3-phosphate dehydrogenase (GAPDH) loading control (2118L, Cell Signalling Technology, Danvers, MA). Enhanced chemiluminescent images were captured using a Bio-Rad ChemiDoc Imaging System (Bio-Rad, Hercules,

CA). Target protein expression was quantified using densitometric analysis.

Oxylipin analysis

At the study endpoint, plasma samples were collected for oxylipin analysis in a subset of mice, as previously described.²¹ Blood samples were collected into ethylenediaminetetraacetic acid-coated blood-collection tubes (Microvette CB 300 K2E, 16.444.100, Sarstedt, Numbrecht, Germany) and centrifuged for 5 minutes at 4°C and 2000 g. The resulting plasma then was stored at -80°C until processing. A total of 97 oxylipins were extracted from prepared plasma samples using Strata-X SPE solid-phase extraction columns (Phenomenex, Torrance, CA) and analyzed by high-performance liquid chromatography—electrospray ionization—tandem mass spectroscopy, as previously described.^{34,35}

Statistical analysis

The statistical software packages SPSS 15.0, SPSS version 24 (both IBM, Armonk, NY), and GraphPad Prism 5 (GraphPad, La Jolla, CA) were utilized to perform the statistical analyses. All data were expressed as mean ± standard deviation, unless otherwise noted. Results with *P* < 0.05 were considered significant. Echocardiographic analyses were performed by analysis of variance (ANOVA) with Dunnett's *post hoc* analysis. Histologic analysis was performed using the Mann-Whitney and Kruskal-Wallis tests for nonparametric comparison of scores among the groups. The scores ranged from 0 to 5, with 0 representing no tissue injury, and 5

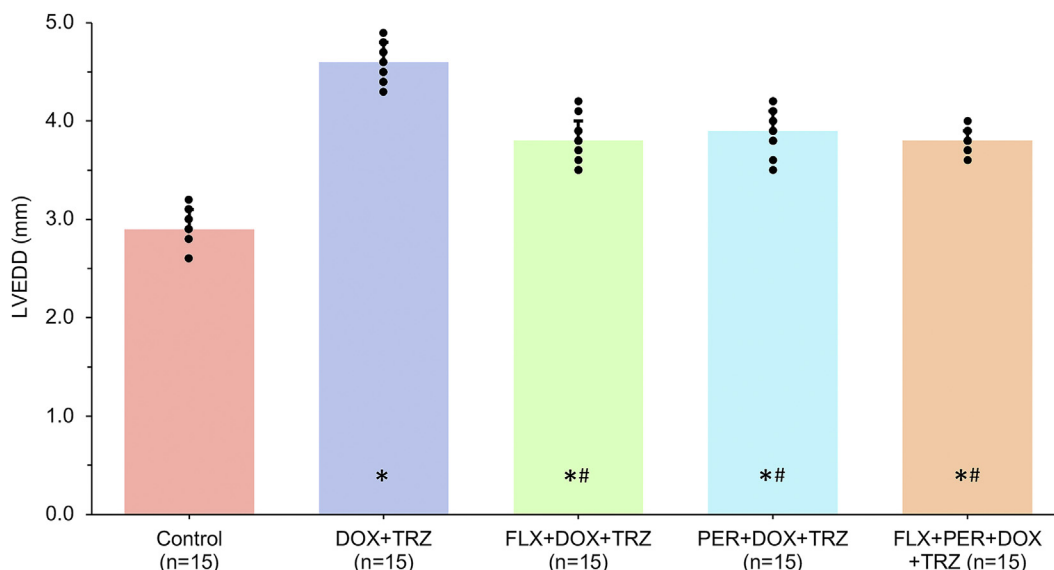


Figure 2. Echocardiographic changes in left ventricular end-diastolic diameter (LVEDD) of mice administered with flaxseed (FLX), perindopril (PER), or FLX + PER after treatment with doxorubicin (DOX) + trastuzumab (TRZ). * $P < 0.05$, DOX + TRZ vs control. *# $P < 0.05$, FLX + DOX + TRZ, or PER + DOX + TRZ, or PER + FLX + DOX + TRZ vs DOX + TRZ and control.

representing severe tissue damage. Western analysis data were expressed as mean \pm standard error of the mean. For *post hoc* analysis, repeated measures of 1-way ANOVA were used to evaluate for significance between independent factors. Statistical significance for the oxidized phospholipid and oxylipin analyses were calculated by 1-way ANOVA followed by a Tukey *post hoc* test.

Results

Murine echocardiography

For all study groups, heart rate and LV wall thickness (interventricular septal wall thickness and posterior wall thickness) were similar at baseline and at week 6. Mice treated with DOX + TRZ demonstrated adverse LV structural remodeling, with an increase in LVEDD from 2.9 ± 0.2 mm at baseline to 4.6 ± 0.2 mm at week 6 ($P < 0.05$). Treatment with either FLX, PER, or FLX + PER improved LV structure, with LVEDD values of 3.8 ± 0.2 mm, 3.9 ± 0.2 mm, and 3.8 ± 0.1 mm, respectively ($P < 0.05$), at study endpoint (Table 1). Treatment with the combination of FLX + PER, however, was not synergistic in reversing LV structural changes (Fig. 2).

Mice treated with DOX + TRZ demonstrated severe LV systolic dysfunction, with a decline in LVEF from $74\% \pm 4\%$ at baseline to $30\% \pm 2\%$ at week 6 ($P < 0.05$). Treatment with either FLX, PER, or FLX + PER improved LV systolic function, with LVEF values of $52\% \pm 4\%$, $54\% \pm 4\%$, and $55\% \pm 3\%$, respectively ($P < 0.05$), at study endpoint (Table 1). Treatment with the combination of FLX + PER, however, was not synergistic in reversing LV systolic dysfunction (Fig. 3). No significant differences were present between any of the groups at the end of the anticancer treatment period (end of week 3) before the recovery period

started (data not shown). No significant difference was present in serial blood pressure measurements among all 5 study groups (data not shown).

Histology

Light microscopy demonstrated normal cardiomyocyte integrity in the control group (Fig. 4A). In mice treated with DOX + TRZ, marked cellular damage and myofibril disarray occurred (Fig. 4B). Treatment with FLX, PER, or FLX + PER reduced these histopathologic changes (Fig. 4, C-E), compared to treatment with DOX + TRZ ($P < 0.05$). No changes in fibrosis were observed among the groups.

Electron microscopy also demonstrated normal cardiomyocyte integrity in the control group (Fig. 5A). In mice treated with DOX + TRZ, myofibril degradation, vacuolization, and loss of sarcomere integrity were increased significantly, compared to the values in the control group ($P < 0.001$; Fig. 5B). Treatment with FLX, PER, or FLX + PER partially reversed these adverse histologic changes (Fig. 5C-E), compared to those in the DOX + TRZ group ($P < 0.05$).

Western blot analyses

In mice treated with DOX + TRZ, a 2.3-fold increase occurred in HMGB1 expression, compared to that in healthy control mice ($P < 0.05$; Fig. 6; Supplemental Fig. S1). Elevations in this biomarker of necrosis and mitochondria-mediated ferroptosis were downregulated significantly in mice treated with FLX, PER, or FLX + PER ($P < 0.05$).

In mice treated with DOX + TRZ, a 2.4-fold increase occurred in Bnip-3 expression, compared to the level in healthy control mice ($P < 0.05$; Fig. 7; Supplemental Fig. S2). Elevations in this biomarker of mitochondrial damage, apoptosis, and necrosis were downregulated significantly in mice treated with FLX, PER, or FLX + PER ($P < 0.05$).

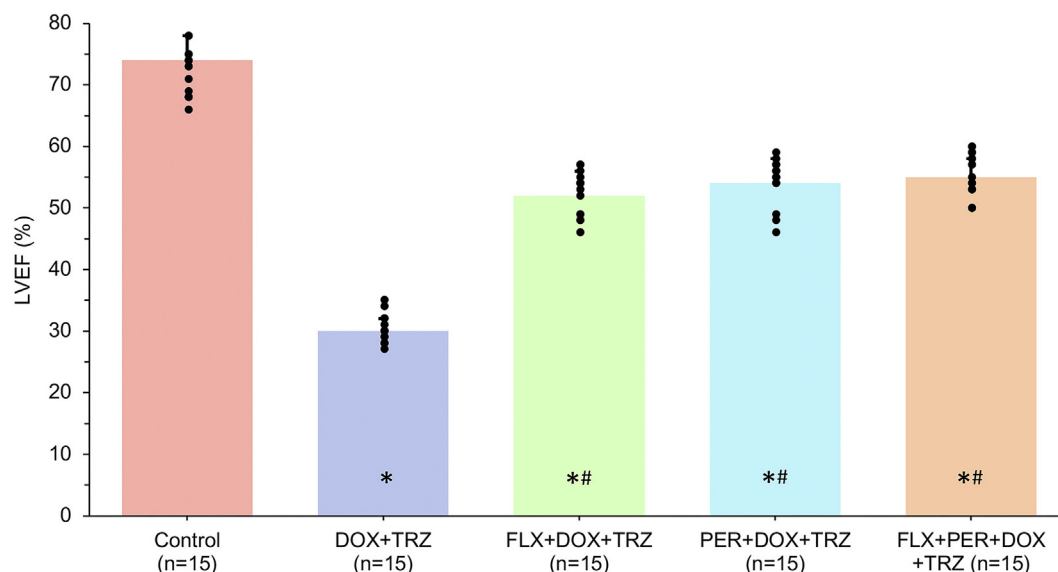


Figure 3. Echocardiographic changes in left ventricular ejection fraction (LVEF) of mice administered with flaxseed (FLX), perindopril (PER), or FLX + PER after treatment with doxorubicin (DOX) + trastuzumab (TRZ). * $P < 0.05$, DOX + TRZ vs control. ** $P < 0.05$, FLX + DOX + TRZ, or PER + DOX + TRZ, or PER + FLX + DOX + TRZ vs DOX + TRZ and control.

No significant difference occurred in NF- κ B, phospho-NF- κ B, poly-adenosine diphosphate (ADP)-ribose-polymerase, Bcl-2 associated X protein, B-cell lymphoma extra-large, or Caspase-3 among all 5 study groups (data not shown).

Oxylipins

In mice treated with DOX + TRZ, a 3.3-fold increase occurred in the concentration of (\pm)18 hydroxyeicosate-trienoic acid (18-HETE), compared to the concentration in healthy control mice ($P < 0.05$; Fig. 8). Elevations in this oxylipin were downregulated significantly in mice treated with FLX, PER, or FLX + PER ($P < 0.05$).

In mice treated with DOX + TRZ, a 7.3-fold increase occurred in the concentration of 20-carboxy-arachidonic acid (20-COOH-AA), compared to the concentration in healthy control mice ($P < 0.05$; Fig. 9). Elevations in this oxylipin were downregulated significantly in mice treated with FLX, PER, or FLX + PER ($P < 0.05$).

Discussion

The evolving field of cardio-oncology applies various therapies, including pharmaceuticals and nutraceuticals, in an attempt to manage and reverse chemotherapy-mediated cardiotoxicity. Although FLX was equivalent to PER in the

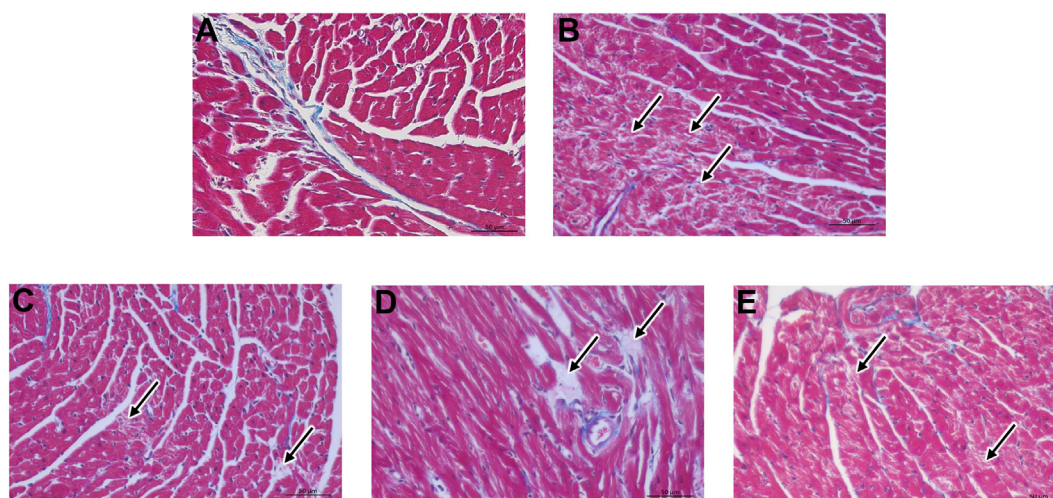


Figure 4. Masson's trichrome–stained light microscopy slides representative of the cardiomyocyte morphology changes for each treatment group. **Arrows** indicate areas of cellular damage and myofibril disarray. The number of arrows correspond to the level of damage. **(A)** Control; **(B)** doxorubicin (DOX) + trastuzumab (TRZ); **(C)** flaxseed (FLX) + DOX + TRZ; **(D)** perindopril (PER) + DOX + TRZ; and **(E)** FLX + PER + DOX + TRZ.

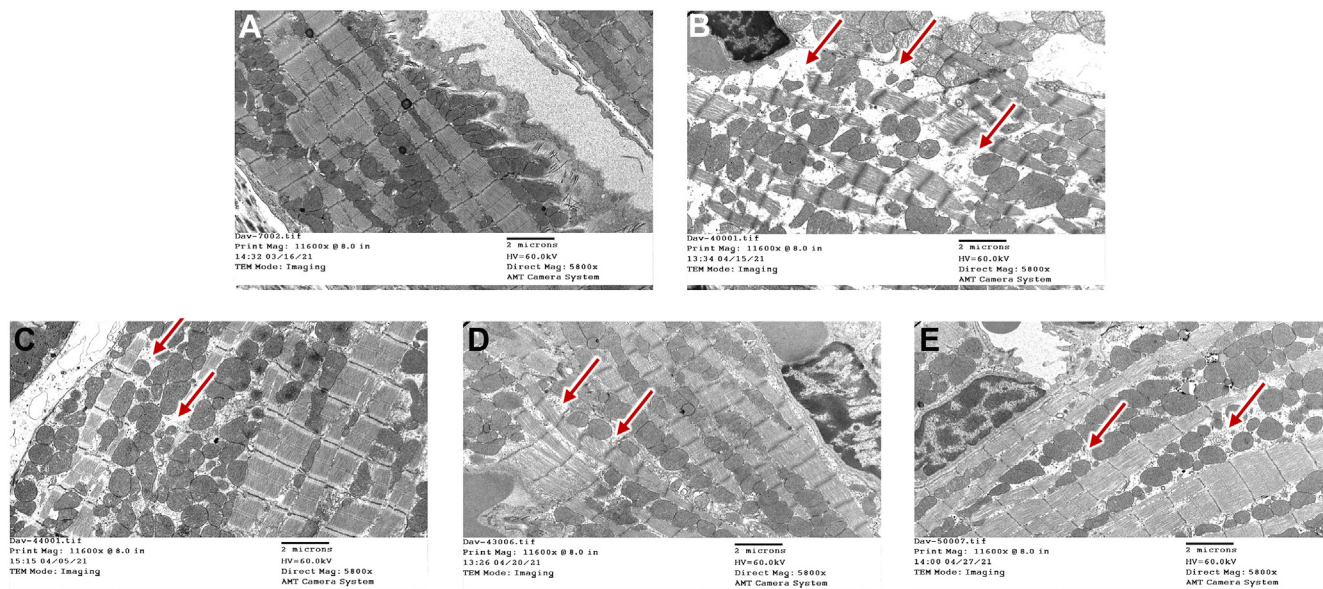


Figure 5. Electron microscopy slides representative of the cardiomyocyte morphology changes for each treatment group. **Arrows** indicate areas of myofibril degradation, vacuolization, and loss of sarcomere integrity. The number of arrows correspond to the level of damage. **(A)** Control; **(B)** doxorubicin (DOX) + trastuzumab (TRZ); **(C)** flaxseed (FLX) + DOX + TRZ; **(D)** perindopril (PER) + DOX + TRZ; and **(E)** FLX + PER + DOX + TRZ.

treatment of adverse LV remodeling in our current chronic *in vivo* murine model of DOX + TRZ-induced cardiotoxicity, the combination of FLX + PER was not synergistic. Our study demonstrated that treating established DOX + TRZ-induced cardiotoxicity with either FLX or PER had the following effects: (i) reversal of adverse LV cavity remodeling; (ii) improvement of myofibrillar disarray and cardiomyocyte vacuolization; (iii) lowering of the expression level of HMGB1, a biomarker of necrosis and mitochondrially mediated ferroptosis; (iv) lowering of the expression level of Bnip-3, a biomarker of mitochondria damage, apoptosis, and necrosis; and (v) reduction of the levels of proinflammatory, profibrotic, and pro-apoptotic oxylipins in a chronic *in vivo* murine model.

FLX and renin-angiotensin system (RAS) antagonism improve adverse cardiovascular remodelling due to DOX + TRZ

The increased morbidity and mortality associated with chemotherapy-mediated cardiotoxicity have necessitated the search for prophylactic agents to prevent these adverse side effects. Promising agents include ACEi and/or angiotensin receptor blockers, β -blockers, statins, antioxidants, and nutraceuticals.^{16,17,20,21,26} Previous murine studies have demonstrated the efficacy of ACEi in both the prevention and treatment of DOX + TRZ-mediated cardiotoxicity in the *in vivo* setting.^{25,36-38} Additionally, we recently demonstrated that the nutraceutical FLX is partially cardioprotective in a chronic *in vivo* female murine model of DOX + TRX-mediated cardiotoxicity, and it offers equal cardioprotection to an ACEi when used in the prophylactic setting.^{20,21} In the current chronic *in vivo* study of established DOX + TRZ-mediated cardiotoxicity, we observed that intervening with either FLX, PER, or FLX + PER improved LV remodeling on both a structural and functional level, with an \sim 18% decrease in LVEDD and an \sim 40% increase in LVEF, compared to the

levels in the control group. As the first murine study to demonstrate the equivalence of FLX and the ACEi PER in the treatment of DOX + TRZ-mediated cardiotoxicity, this raises the question of whether nutraceuticals can be used in lieu of and/or in combination with pharmaceuticals for the management of CTRCD in the clinical setting.

FLX and RAS antagonism improve adverse histologic changes due to DOX + TRZ

DOX and TRZ both have been associated with similar histopathologic changes, including loss of cardiomyocyte integrity through mitochondrial swelling, vacuolization, and myofibrillar degeneration.^{20,25,39-46} These pathologic changes, however, may be prevented through the prophylactic administration of RAS antagonists and nutraceutical agents.^{36,38,47} Recently, we demonstrated that the prophylactic administration of FLX and PER were equivalent in attenuating DOX + TRZ-induced loss of cellular integrity, myofibril disarray, and vacuolization.²¹ To corroborate these findings, the current study revealed significant improvement of DOX + TRZ-induced myocyte damage in all 3 experimental groups, using treatment with PER, FLX, or FLX + PER. This result demonstrates that the histopathologic changes of DOX + TRZ-mediated cardiac injury can be reversed.

FLX and RAS antagonism inhibit cardiotoxic mechanistic pathways of DOX + TRZ

Mitochondrially mediated ferroptosis. One of the primary mechanisms of DOX-mediated cardiotoxicity is mitochondrial-induced ferroptosis.^{12,48} In the presence of iron, oxidative stress causes ferrous and ferric cations to accumulate in the mitochondria, which reduces the mitochondrial membrane potential.^{12,48} Without the necessary membrane potential, cardiomyocyte mitochondria cannot

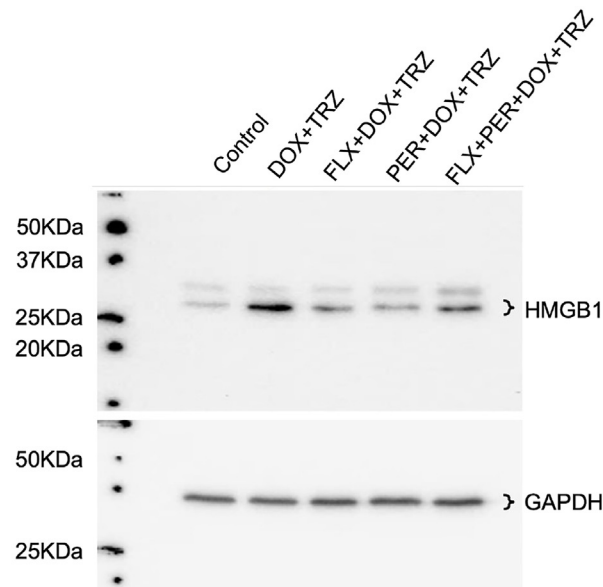
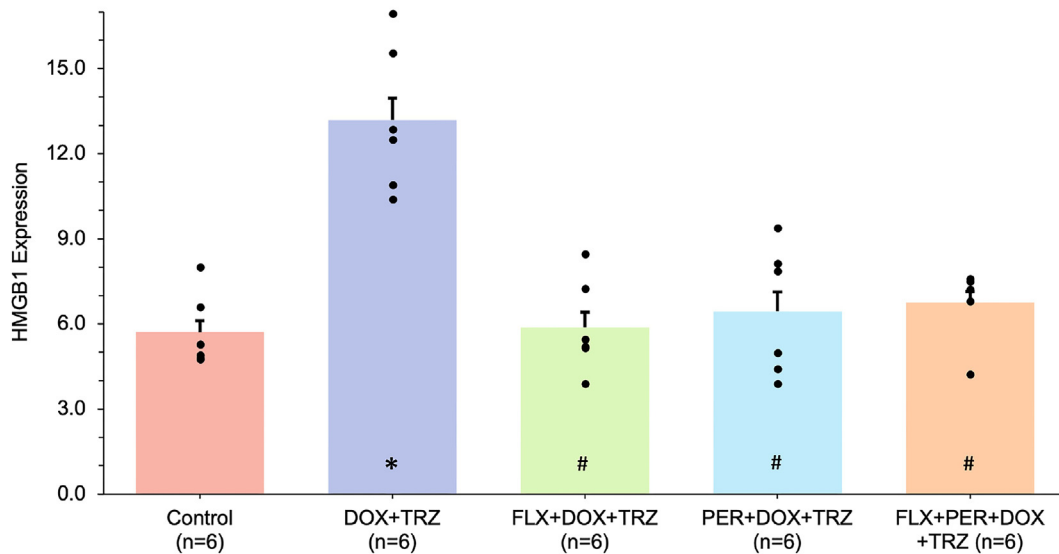
A**B**

Figure 6. Western blot expression of high-mobility group box 1 protein (HMGB1). GAPDH, glyceraldehyde 3-phosphate dehydrogenase. **(A)** Representative Western gel blot; **(B)** Western blot protein expression. * $P < 0.05$, doxorubicin (DOX) + trastuzumab (TRZ) vs control. # $P < 0.05$, flaxseed (FLX) + DOX + TRZ, or perindopril (PER) + DOX + TRZ, or PER + FLX + DOX + TRZ vs DOX + TRZ. For original Western blot images, see [Supplemental Appendix S1](#).

maintain the energy production required for repetitive myocyte contractions. This iron-induced energy crisis triggers a preprogrammed ferroptotic cell-death pathway.

In the current study, DOX + TRZ–induced ferroptosis via iron accumulation in the mitochondria is reflected by the increase in HMGB1 expression. Of interest, HMGB1 expression was attenuated to the level of healthy controls in mice treated with FLX, PER, or FLX + PER. Our results suggest that FLX and PER arrested the progression of ferroptosis in the 3 experimental groups, allowing the cardiomyocytes to recover instead of completing the cell-death

pathway. Although the increase in HMGB1 levels in the DOX + TRZ group aligns with findings in the established literature,^{12-14,48} the attenuation of HMGB1 by FLX and PER is a novel discovery that adds to the established evidence that antioxidants can temper the cardiotoxic side effects of DOX by reducing cell death.

Mitochondrially mediated apoptosis and necrosis. In addition to ferroptosis, DOX also has been established to induce mitochondrial dysfunction via upregulation of Bnip-3.¹⁰ In both *in vitro* and *in vivo* models, DOX causes dose-

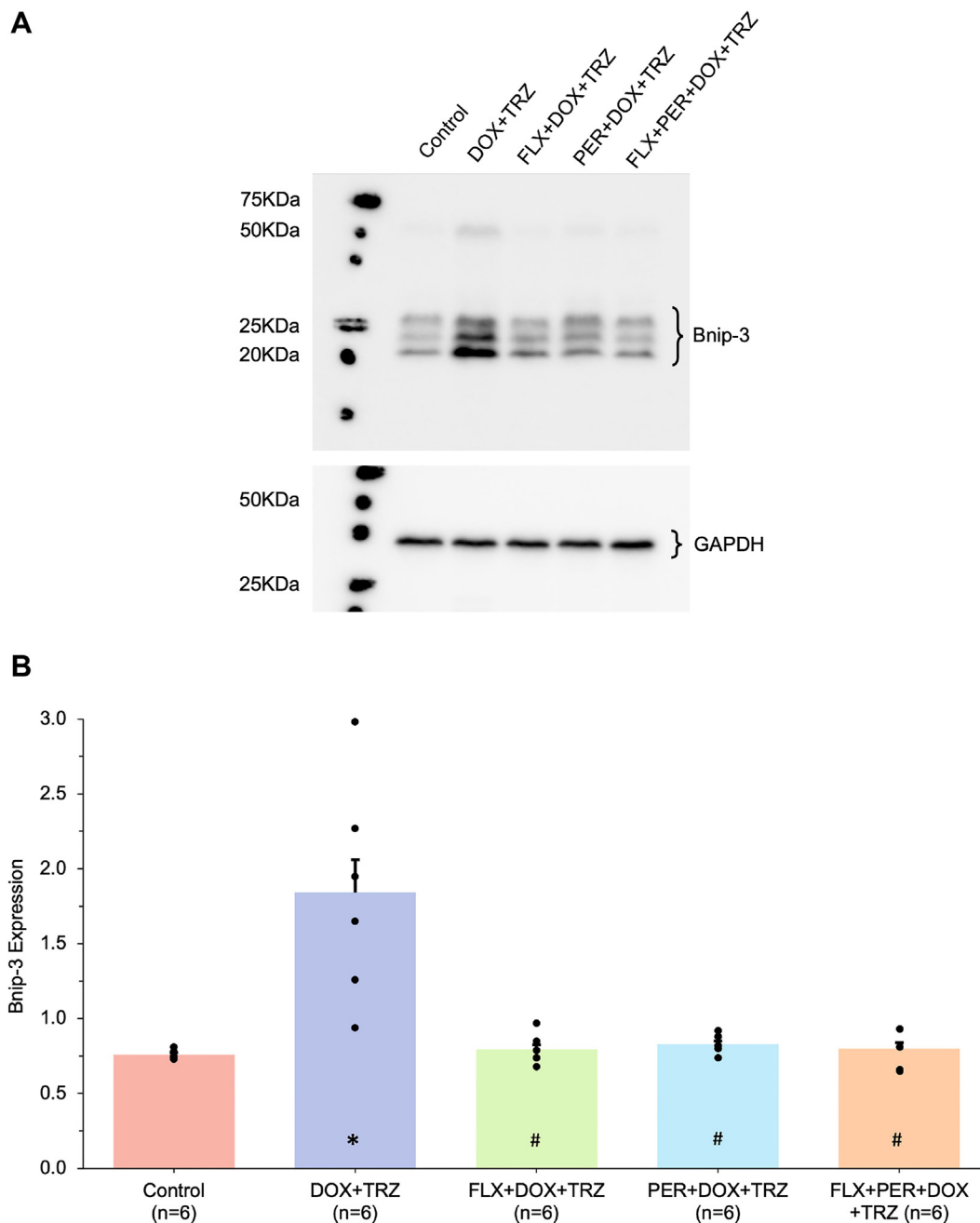


Figure 7. Western blot expression of B-cell lymphoma 2 interacting protein 3 (Bnip-3). GAPDH, glyceraldehyde 3-phosphate dehydrogenase. **(A)** Representative Western gel blot; **(B)** Western blot protein expression. * $P < 0.05$, doxorubicin (DOX) + trastuzumab (TRZ) vs control. # $P < 0.05$, flaxseed (FLX) + DOX + TRZ, or perindopril (PER) + DOX + TRZ, or PER + FLX + DOX + TRZ vs DOX + TRZ. For original Western blot images, see [Supplemental Appendix S1](#)

dependent upregulation of cardiomyocyte Bnip-3 expression. Bnip-3 then induces mitochondrial injury by degrading the mitochondrial membranes, thus disrupting the energy production required for repetitive myocyte contractions. The resulting energy crisis triggers apoptotic or necrotic cell-death pathways. However, inhibition of Bnip-3 can restore mitochondrial respiration and offer resistance against the misaligned sarcomeres and vacuolization typically induced by DOX.¹⁰

In the present study, we demonstrated that Bnip-3 expression was increased 2.3-fold in mice treated with

DOX + TRZ. However, treatment with either FLX, PER, or the combination of FLX + PER attenuated Bnip-3 to the same levels as in the healthy controls. These effects likely are due to the antioxidative properties of FLX and PER.^{10-14,20,48,49} In the DOX + TRZ group, oxidative stress upregulates Bnip-3, compromising the integrity of the mitochondria. This effect caused cardiomyocytes to enter an energy crisis and initiate apoptotic and necrotic cell-death pathways, ultimately leading to functional changes in the heart. In the 3 experimental groups, however, the antioxidant

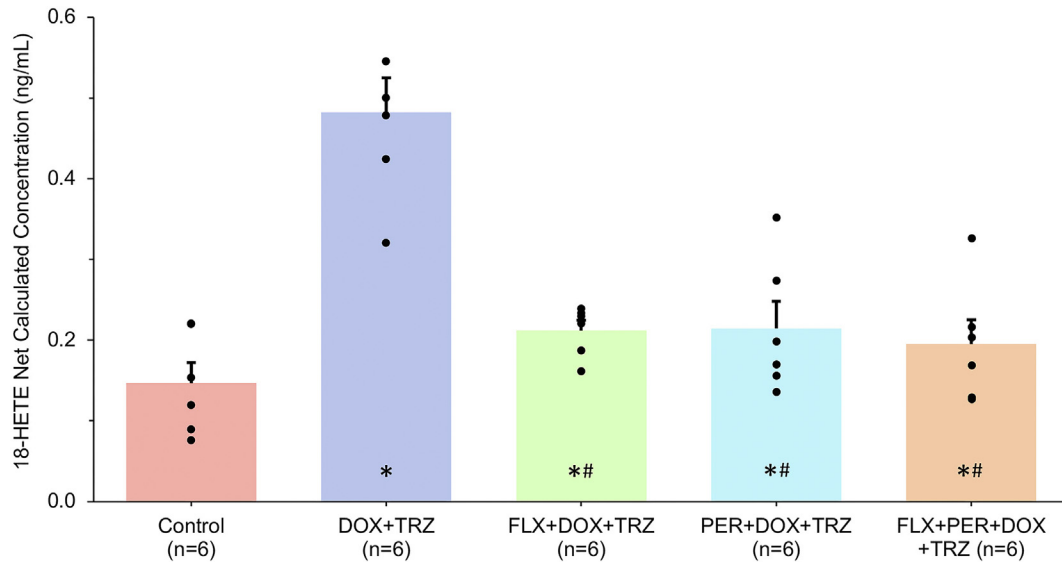


Figure 8. Oxylipin (\pm)18 hydroxyeicosatetraenoic acid (18-HETE) concentration. * $P < 0.05$, doxorubicin (DOX) + trastuzumab (TRZ) vs control. *# $P < 0.05$, flaxseed (FLX) + DOX + TRZ, or perindopril (PER) + DOX + TRZ, or PER + FLX + DOX + TRZ vs DOX + TRZ and control.

properties of PER and FLX attenuated the oxidative stress, thus protecting the mitochondria and preventing apoptosis and necrosis in the cardiomyocytes. The presence of necrotic cells also is supported by the altered HMGB1 expression, as, in addition to indicating ferroptosis, HMGB1 is released passively from necrotic cells.¹¹ Further studies, however, are warranted to elucidate the relative contributions of mitochondrial damage and the various associated cell-death pathways in the development of CTRCD.

Inflammatory changes in DOX + TRZ-mediated cardiotoxicity. In addition to inducing changes in the expression of proteins involved in ferroptosis, apoptosis, and necrosis, DOX + TRZ can elicit changes in lipid

metabolism.⁵⁰ Generated through polyunsaturated fatty acid (PUFA) oxidation, oxylipins are active metabolites that can be produced via the cytochrome P450 (CYP) pathway.^{50,51} The CYP ω -hydroxylase pathway produces hydroxy-eicosatetraenoic acids (HETEs) from arachidonic acid that are highly expressed in cardiomyocytes.⁵² HETEs also can be further metabolized, as seen in the conversion of 20-HETE into 20-COOH-AA. Although CYP ω -hydroxylase-derived HETEs and their metabolites have been associated with proinflammatory, profibrotic, and pro-apoptotic effects, 18-HETE and 20-HETE synthesis also have been shown to be upregulated in models of DOX-induced cardiotoxicity.⁵⁰⁻⁵²

In our current study, DOX + TRZ-mediated oxidative stress caused upregulation of the oxylipins 18-HETE and

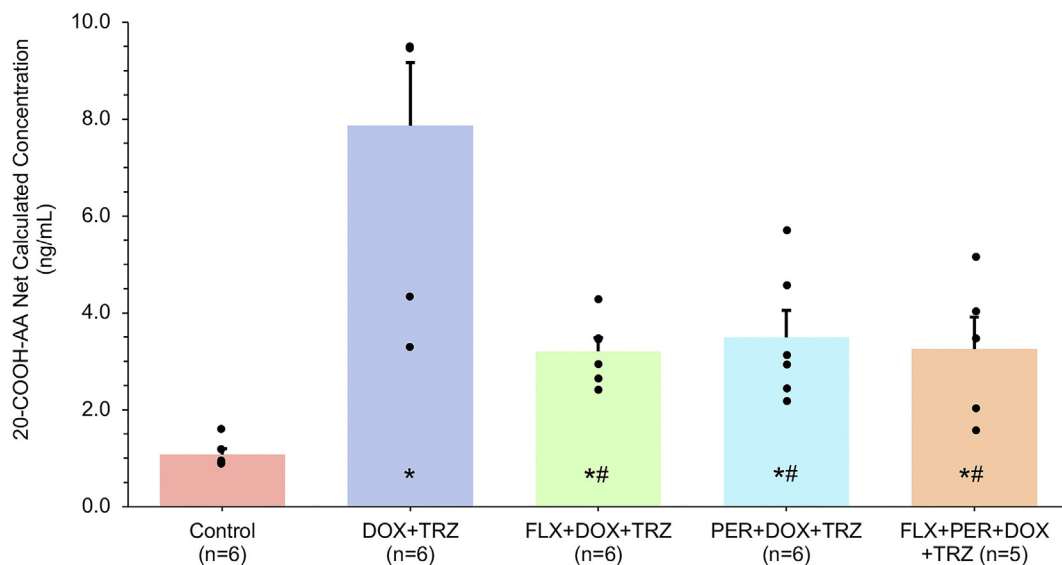


Figure 9. Oxylipin 20-carboxy-arachidonic acid (20-COOH-AA) concentration. * $P < 0.05$, doxorubicin (DOX) + trastuzumab (TRZ) vs control. *# $P < 0.05$, flaxseed (FLX) + DOX + TRZ, or perindopril (PER) + DOX + TRZ, or PER + FLX + DOX + TRZ vs DOX + TRZ and control.

20-COOH-AA. This effect may have caused inflammation and apoptosis leading to cardiac fibrosis and heart failure. As elevations in these oxylipins were downregulated significantly in mice treated with FLX, PER, or FLX + PER, this may have improved adverse cardiovascular remodelling due to DOX + TRZ in our *in vivo* model. Further, due to the increased angiogenesis and tumour proliferation associated with CYP ω -hydroxylase oxylipins, FLX also may exhibit anticancer effects by attenuating this pathway.⁵⁰ Considering the possible anticancer effects of FLX, in addition to its cardioprotective effects, further research is required to explore these metabolic lipid pathways in the field of cardio-oncology.

A number of limitations are associated with the current study. First, although DOX + TRZ were administered concurrently to create a robust model of chemotherapy-mediated cardiotoxicity,^{20,21} these anticancer agents typically are administered sequentially in the clinical setting. Further research is warranted to characterize DOX + TRZ-mediated cardiotoxicity and the possible treatment effects of FLX and PER, via administration of the anticancer agents sequentially. Second, the chronic *in vivo* murine model for the current study consisted entirely of female mice. As breast cancer and its associated use of cardiotoxic anticancer therapies are not exclusive to female patients, further research is warranted to evaluate the cardiovascular treatment potential of FLX and PER in male models. Third, although only LV cavity dimensions and systolic function were acquired, we will incorporate noninvasive diastolic parameters in future studies. Finally, the current study did not evaluate whether FLX or PER has an impact on the antineoplastic properties of DOX + TRZ. Further research is warranted to ensure that treatment with FLX and PER does not have a negative impact on the anticancer effects of DOX + TRZ.

Conclusions

FLX was equivalent to PER at improving cardiovascular remodelling by reducing biomarkers of inflammation, mitochondrial damage, and cell death; however, the combination of FLX + PER was not synergistic. Future clinical studies are warranted to investigate whether FLX consumption is equivalent to PER in reversing the cardiotoxic side effect of DOX + TRZ in women with breast cancer.

Acknowledgements

All work related to this study was performed at the St. Boniface Hospital Albrechtsen Research Centre and the University of Manitoba.

Ethics Statement

The guidelines of the Canadian Council on Animal Care were followed for all animal procedures, including drug administrations and longitudinal echocardiographic studies, as approved by the Animal Protocol Review Committee at the University of Manitoba (REB: 20-004/1 [AC11548]).

Patient Consent

The authors confirm that patient consent is not applicable to this article. This is a preclinical trial using a murine model;

therefore, no patients were involved who could be required to give consent.

Funding Sources

Support was provided by the Heart and Stroke Foundation of Canada (grant number G-19-0024241) to D.S.J.; Canadian Institutes of Health Research Canada Graduate Scholarship- Masters and University of Manitoba Rady Faculty of Health Sciences Graduate Scholarship to S.M.T-L.; and at University of Manitoba (Winnipeg, Manitoba, Canada), a Rady Faculty of Health Sciences Graduate Studentship to S.M.T-L., and a Naranjan Dhalla Chair in Cardiovascular Research supported by the St. Boniface Hospital and Research Foundation to P.K.S.

Disclosures

The authors have no conflicts of interest to disclose.

References

1. Anampa J, Makower D, Sparano JA. Progress in adjuvant chemotherapy for breast cancer: an overview. *BMC Med* 2015;13:195.
2. Cancer Care Ontario. AC-PACL(DD) patient information. Available at: <https://www.cancercareontario.ca/en/drugformulary/regimens/infosheet/46136>. Accessed July 6, 2022.
3. Altena R, Perik PJ, van Veldhuisen DJ, de Vries EG, Gietema JA. Cardiovascular toxicity caused by cancer treatment: strategies for early detection. *Lancet Oncol* 2009;10:391-9.
4. Singal PK, Iliskovic N. Doxorubicin-induced cardiomyopathy. *N Engl J Med* 1998;339:900-5.
5. Slamon DJ, Leyland-Jones B, Shak S, et al. Use of chemotherapy plus a monoclonal antibody against HER2 for metastatic breast cancer that overexpresses HER2. *N Engl J Med* 2001;344:783-92.
6. McArthur HL, Chia S. Cardiotoxicity of trastuzumab in clinical practice. *N Engl J Med* 2007;357:94-5.
7. Guglin M, Hartlage G, Reynolds C, Chen R, Patel V. Trastuzumab-induced cardiomyopathy: not as benign as it looks? A retrospective study. *J Card Fail* 2009;15:651-7.
8. Wadhwa D, Fallah-Rad N, Grenier D, et al. Trastuzumab mediated cardiotoxicity in the setting of adjuvant chemotherapy for breast cancer: a retrospective study. *Breast Cancer Res Treat* 2009;117:357-64.
9. Akolkar G, da Silva Dias D, Ayyappan P, et al. Vitamin C mitigates oxidative/nitrosative stress and inflammation in doxorubicin-induced cardiomyopathy. *Am J Physiol Heart Circ Physiol* 2017;313:H795-809.
10. Dhingra R, Margulets V, Chowdhury SR, et al. Bnip3 mediates doxorubicin-induced cardiac myocyte necrosis and mortality through changes in mitochondrial signaling. *Proc Natl Acad Sci U S A* 2014;111: E5537-44.
11. Yao Y, Xu X, Zhang G, et al. Role of HMGB1 in doxorubicin-induced myocardial apoptosis and its regulation pathway. *Basic Res Cardiol* 2012;107:267.
12. Zhang H, Wang Z, Liu Z, Du K, Lu X. Protective effects of dexazoxane on rat ferroptosis in doxorubicin-induced cardiomyopathy through regulating HMGB1. *Front Cardiovasc Med* 2021;8:685434.

13. Kitakata H, Endo J, Ikura H, et al. Therapeutic targets for DOX-induced cardiomyopathy: role of apoptosis vs. ferroptosis. *Int J Mol Sci* 2022;23:1414.
14. Tadokoro T, Ikeda M, Ide T, et al. Mitochondria-dependent ferroptosis plays a pivotal role in doxorubicin cardiotoxicity. *JCI Insight* 2020;5:e132747.
15. Rahman GA. Breast conserving therapy: a surgical technique where little can mean more. *J Surg Tech Case Rep* 2011;3:1-4.
16. Virani SA, Dent S, Brezden-Masley C, et al. Canadian Cardiovascular Society guidelines for evaluation and management of cardiovascular complications of cancer therapy. *Can J Cardiol* 2016;32:831-41.
17. Hamo CE, Bloom MW, Cardinale D, et al. Cancer therapy-related cardiac dysfunction and heart failure: part 2: prevention, treatment, guidelines, and future directions. *Circ Heart Fail* 2016;9:e002843.
18. Plana JC, Galderisi M, Barac A, et al. Expert consensus for multimodality imaging evaluation of adult patients during and after cancer therapy: a report from the American Society of Echocardiography and the European Association of Cardiovascular Imaging. *Eur Heart J Cardiovasc Imaging* 2014;15:1063-93.
19. Boon HS, Olatunde F, Zick SM. Trends in complementary/alternative medicine use by breast cancer survivors: comparing survey data from 1998 and 2005. *BMC Womens Health* 2007;7:4.
20. Asselin CY, Lam A, Cheung DYC, et al. The cardioprotective role of flaxseed in the prevention of doxorubicin- and trastuzumab-mediated cardiotoxicity in C57BL/6 mice. *J Nutr* 2020;150:2353-63.
21. Eekhoudt CR, Bortoluzzi T, Varghese SS, et al. Comparing flaxseed and perindopril in the prevention of doxorubicin and trastuzumab-induced cardiotoxicity in C57BL/6 mice. *Curr Oncol* 2022;29:2941-53.
22. Milano G, Raucci A, Scopece A, et al. Doxorubicin and trastuzumab regimen induces biventricular failure in mice. *J Am Soc Echocardiogr* 2014;27:568-79.
23. Bosch X, Rovira M, Sitges M, et al. Enalapril and carvedilol for preventing chemotherapy-induced left ventricular systolic dysfunction in patients with malignant hemopathies: the OVERCOME trial (prevention of left ventricular dysfunction with Enalapril and carvedilol in patients submitted to intensive Chemotherapy for the treatment of Malignant hemopathies). *J Am Coll Cardiol* 2013;61:2355-62.
24. Flower G, Fritz H, Balneaves LG, et al. Flax and breast cancer: a systematic review. *Integr Cancer Ther* 2014;13:181-92.
25. Akolkar G, Bhullar N, Bews H, et al. The role of renin angiotensin system antagonists in the prevention of doxorubicin and trastuzumab induced cardiotoxicity. *Cardiovasc Ultrasound* 2015;13:18.
26. Akolkar G, Bagchi AK, Ayyappan P, Jassal DS, Singal PK. Doxorubicin-induced nitrosative stress is mitigated by vitamin C via the modulation of nitric oxide synthases. *Am J Physiol Cell Physiol* 2017;312:C418-27.
27. Dessì M, Piras A, Madeddu C, et al. Long-term protective effects of the angiotensin receptor blocker telmisartan on epirubicin-induced inflammation, oxidative stress and myocardial dysfunction. *Exp Ther Med* 2011;2:1003-9.
28. Cardinale D, Colombo A, Sandri MT, et al. Prevention of high-dose chemotherapy-induced cardiotoxicity in high-risk patients by angiotensin-converting enzyme inhibition. *Circulation* 2006;114:2474-81.
29. Kalam K, Marwick TH. Role of cardioprotective therapy for prevention of cardiotoxicity with chemotherapy: a systematic review and meta-analysis. *Eur J Cancer* 2013;49:2900-9.
30. Ludke A, Akolkar G, Ayyappan P, Sharma AK, Singal PK. Time course of changes in oxidative stress and stress-induced proteins in cardiomyocytes exposed to doxorubicin and prevention by vitamin C. *PLoS One* 2017;12:e0179452.
31. Walker JR, Sharma A, Lytwyn M, et al. The cardioprotective role of probucol against anthracycline and trastuzumab-mediated cardiotoxicity. *J Am Soc Echocardiogr* 2011;24:699-705.
32. Ahmadi R, Santiago JJ, Walker J, et al. A high-lipid diet potentiates left ventricular dysfunction in nitric oxide synthase 3-deficient mice after chronic pressure overload. *J Nutr* 2010;140:1438-44.
33. Luft JH. Improvements in epoxy resin embedding methods. *J Biophys Biochem Cytol* 1961;9:409-14.
34. Aukema HM, Winter T, Ravandi A, et al. Generation of bioactive oxylipins from exogenously added arachidonic, eicosapentaenoic and docosahexaenoic acid in primary human brain microvessel endothelial cells. *Lipids* 2016;51:591-9.
35. Leng S, Winter T, Aukema HM. Dietary LA and sex effects on oxylipin profiles in rat kidney, liver, and serum differ from their effects on PUFAs. *J Lipid Res* 2017;58:1702-12.
36. Hiona A, Lee AS, Nagendran J, et al. Pretreatment with angiotensin-converting enzyme inhibitor improves doxorubicin-induced cardiomyopathy via preservation of mitochondrial function. *J Thorac Cardiovasc Surg* 2011;142:396-403.e3.
37. Zhang YC, Tang Y, Zhang M, et al. Fosinopril attenuates the doxorubicin-induced cardiomyopathy by restoring the function of sarcoplasmic reticulum. *Cell Biochem Biophys* 2012;64:205-11.
38. Soga M, Kamal FA, Watanabe K, et al. Effects of angiotensin II receptor blocker (candesartan) in daunorubicin-induced cardiomyopathic rats. *Int J Cardiol* 2006;110:378-85.
39. Goyal V, Bews H, Cheung D, et al. The cardioprotective role of N-acetyl cysteine amide in the prevention of doxorubicin and trastuzumab-mediated cardiac dysfunction. *Can J Cardiol* 2016;32:1513-9.
40. Parikh M, Raj P, Austria JA, et al. Dietary flaxseed protects against ventricular arrhythmias and left ventricular dilation after a myocardial infarction. *J Nutr Biochem* 2019;71:63-71.
41. Shapira J, Gotfried M, Lishner M, Ravid M. Reduced cardiotoxicity of doxorubicin by a 6-hour infusion regimen. A prospective randomized evaluation. *Cancer* 1990;65:870-3.
42. Siveski-Iliskovic N, Kaul N, Singal PK. Probucol promotes endogenous antioxidants and provides protection against adriamycin-induced cardiomyopathy in rats. *Circulation* 1994;89:2829-35.
43. Rea D, Coppola C, Barbieri A, et al. Strain analysis in the assessment of a mouse model of cardiotoxicity due to chemotherapy: sample for pre-clinical research. *In Vivo* 2016;30:279-90.
44. Argun M, Üzümlü K, Sönmez MF, et al. Cardioprotective effect of metformin against doxorubicin cardiotoxicity in rats. *Anatol J Cardiol* 2016;16:234-41.
45. Laird-Fick HS, Tokala H, Kandola S, et al. Early morphological changes in cardiac mitochondria after subcutaneous administration of trastuzumab in rabbits: possible prevention with oral selenium supplementation. *Cardiovasc Pathol* 2020;44:107159.
46. Kertmen N, Aksoy S, Uner A, et al. Which sequence best protects the heart against trastuzumab and anthracycline toxicity? An electron microscopy study in rats. *Anticancer Res* 2015;35:857-64.

47. Sakr HF, Abbas AM, Elsamanoudy AZ. Effect of valsartan on cardiac senescence and apoptosis in a rat model of cardiotoxicity. *Can J Physiol Pharmacol* 2016;94:588-98.
48. Fang X, Wang H, Han D, et al. Ferroptosis as a target for protection against cardiomyopathy. *Proc Natl Acad Sci U S A* 2019;116:2672-80.
49. Telles-Langdon SM, Arya V, Jassal DS. Renin angiotensin system in cancer, lung, liver and infectious diseases. Available at: <https://link.springer.com/book/9783031236204>. Accessed March 14, 2023.
50. Wang B, Wu L, Chen J, et al. Metabolism pathways of arachidonic acids: mechanisms and potential therapeutic targets. *Signal Transduct Target Ther* 2021;6:94.
51. Gabbs M, Leng S, Devassy JG, Monirujaman M, Aukema HM. Advances in our understanding of oxylipins derived from dietary PUFAs. *Adv Nutr* 2015;6:513-40.
52. Alaeddine LM, Harb F, Hamza M, et al. Pharmacological regulation of cytochrome P450 metabolites of arachidonic acid attenuates cardiac injury in diabetic rats. *Transl Res* 2021;235:85-101.

Supplementary Material

To access the supplementary material accompanying this article, visit *CJC Open* at <https://www.cjopen.ca/> and at <https://doi.org/10.1016/j.cjco.2024.03.009>.